Technical Physics Letters, Vol. 28, No. 7, 2002, pp. 560–563. Translated from Pis'ma v Zhurnal Tekhnicheskoĭ Fiziki, Vol. 28, No. 13, 2002, pp. 57–66.

Bicoherent Wavelet Analysis of the Structure Formation in an Electron Beam with Virtual Cathode

A. E. Khramov[a], A. A. Koronovskiĭ[a], and Yu. I. Levin[b]

[a] *Saratov State University, Saratov, Russia*

[b] *State Scientific Center "College", Saratov, Russia*

e-mail: aeh@cas.ssu.runnet.ru

Received December 10, 2001

Abstract—The supercritical electron beam structure formation in a diode gap with inhomogeneous ion background density were analyzed by the bicoherent wavelet transformation method. By studying the wavelet bicoherency of the spatiotemporal data about oscillations in the system, it is possible to effectively reveal and analyze local spatial structures formed in the electron beam. *© 2002 MAIK "Nauka/Interperiodica".*

Study of the complicated chaotic behavior of distributed systems requires using special methods for analysis of the dynamics of coherent structures, since classical linear methods of analysis (for example, spectral) do not provide maximum information about processes taking place in nonlinear systems. Below we consider application of the bicoherent wavelet transformation, a nonlinear method originally proposed in [1], to an analysis of complicated processes in distributed systems.

Developed quite recently, the wavelet analysis offers a powerful method for studying the dynamics of distributed systems and draws increasing attention of researchers [2–4]. Using this method, it is possible to resolve the dynamics on various scale levels representing the structure of signals. The wavelet transform eliminates the need of expanding signals into harmonic series, which is the main disadvantage of the Fourier transformation applied to the analysis of turbulence and chaos because nonlinear equations describing such complicated phenomena in distributed systems possess no intrinsic harmonic modes.

Bisector (bicoherent) representation characterizes phase relationships (phase coupling) between various frequency components of a signal. We can speak of a phase coupling when the analyzed signal simultaneously contains two frequencies, ω_1 and ω_2, the sum (or difference) of which, as well as the sum of the corresponding phases ϕ_1 and ϕ_2 remain constant over a certain period of time. Using bicoherent wavelets, it is possible to reveal the intrinsic structure of spatial and temporal data, determined by the phase coupling, and study the time variation of this structure.

The mutual wavelet bispectrum (wavelet bicoherency) is defined as

$$B_{hg}(f_1, f_2) = \int_T W_h^*(f, \tau) W_g(f_1, \tau) W_g(f_2, \tau) d\tau, \quad (1)$$

where f, f_1, and f_2 are the frequencies obeying a relationship of the type $f = f_1 + f_2$; $h(t)$ and $g(t)$ are the analyzed signals; W_h and W_g are the corresponding wavelet spectra of these signals [2, 4]; T is the time interval for which the mutual wavelet bispectrum is analyze;, and the asterisk denotes a complex conjugate. The wavelet bispectrum is a measure of the phase coupling over the time interval T, which is manifested between components of the wavelet spectrum of the $g(t)$ signal on a time scale of $1/f_1$ and $1/f_2$ and the $h(t)$ signal on a time scale of $1/f$.

An important characteristic of the bicoherent wavelet transformation is the bicoherency sum defined as

$$B_\Sigma(f) = \sqrt{\frac{1}{N_f}\sum (B_{hg}(f_1, f_2))^2}, \quad (2)$$

where summation is performed over all frequencies f_1 and f_2 obeying the condition $f = f_1 + f_2$; N_f is the number of terms in the sum. Also introduced is the total bicoherency defined as

$$B = \sqrt{\frac{1}{N}\sum\sum (B_{hg}(f_1, f_2))^2}, \quad (3)$$

where the sum is taken over all analyzed frequencies f_1 and f_2, N being the total number of terms in this sum.

In this study, we apply the bicoherent wavelet transformation to analysis of the formation and interaction of coherent structures in an electron beam with virtual cathode (VC) in a diode gap with inhomogeneous ion

1063-7850/02/2807-0560$22.00 © 2002 MAIK "Nauka/Interperiodica"

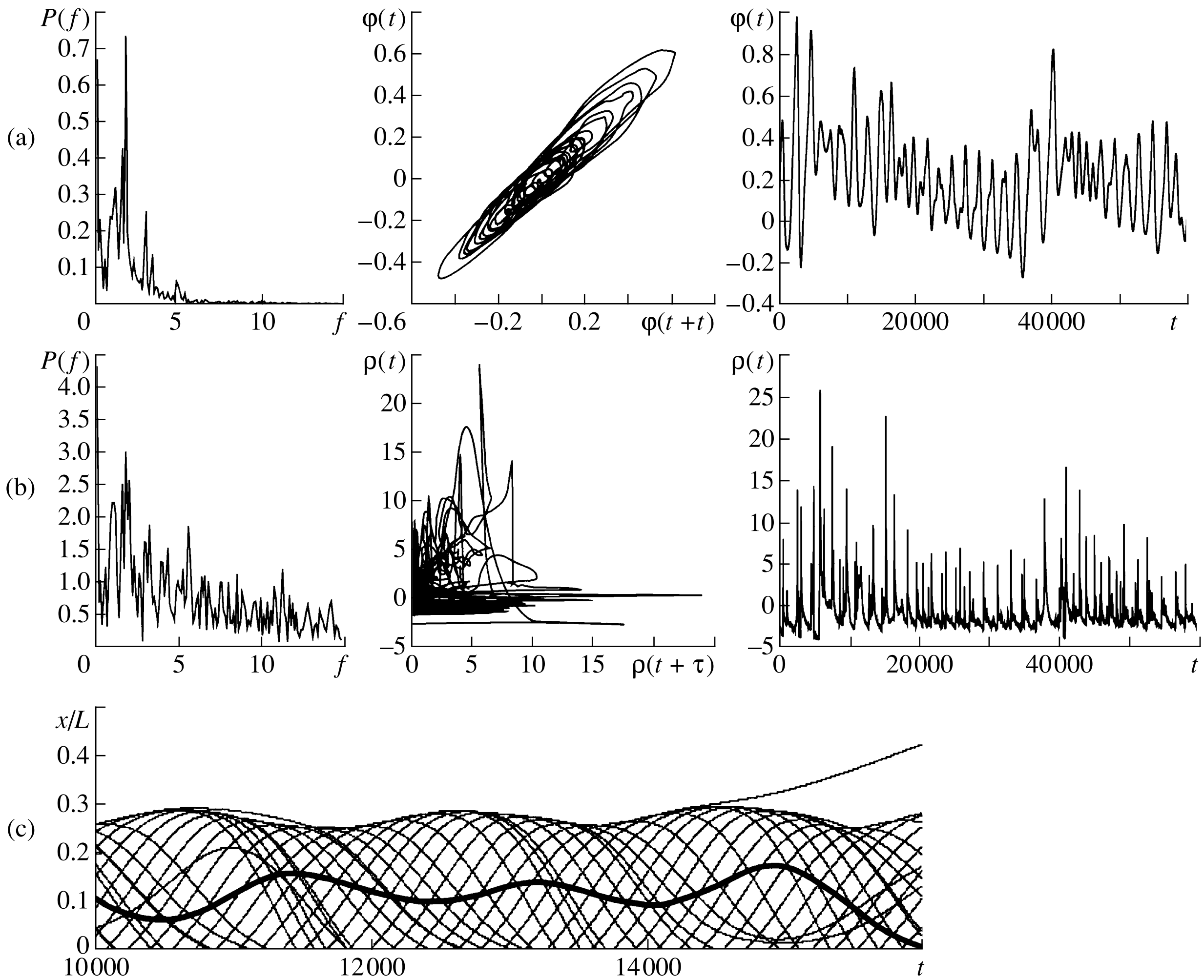

Fig. 1. The power spectra $P(f)$, phase portraits, and time patterns of (a) the electric field potential ϕ and(b) space charge density ρ in the diode gap section with a coordinate $x = 0.25L$; (c) spatiotemporal pattern of the electron flow dynamics in the case studied (thick solid curve represents the trajectory of a particle trapped in a potential well).

background, which was studied in detail previously [5, 6]. This system offers the simplest model of a vircator with plasma anode [7] which allows, under certain conditions, to increase the VC generation frequency [5]. It was demonstrated [6] that the system exhibits a complicated chaotic dynamics of the electron beam.

The system under consideration represents a diode gap with strongly inhomogeneous distribution of an immobile ion background in a region near the injection plane (anode plasma). The control quantities are the Pierce parameter $\alpha = \omega_p L/v_0$ (proportional to the beam current), the ratio $n = \rho_p/\rho_0$ of the anode plasma density ρ_p to the space charge density ρ_0 of the electron beam, and the coordinates x_{p1} (beginning) and x_{p2} (end) of the anode plasma layer; ω_p is the plasma frequency of the electron beam, L is the length of the interaction space, and v_0 is the unperturbed electron flow velocity. For $\alpha > \alpha_{cr}$, a single-stream state of the beam becomes unstable with respect to small perturbations in the charge density and the system features the VC formation [8]. Nonstationary processes in the system were analyzed by a numerical method of macroparticles [9, 10].

As was demonstrated previously [5, 6], the system under consideration exhibits a large set of dynamic regimes depending on the density n of the near-anode ion background and the beam current parameter α. When the ion density exceeds a certain critical value n_{cr} (depending on the Pierce parameter), the system exhibits a transition from regular and weakly stochastic VC oscillations via intermittency to developed chaotic oscillations with a base frequency significantly higher that of the VC oscillations at $n < n_{cr}$. For a significantly inhomogeneous ion background with $n > 2.5$–3.5, the system is characterized by irregular oscillations with a continuous spectrum exhibiting no selected frequency components.

Below we consider a system with the following values of the control parameters: $\alpha = 2.125\pi$, $n = 4.0$, $x_{p1} = 0.05$, and $x_{p2} = 0.25$. The system with these characteristics exhibits a developed spatiotemporal pattern

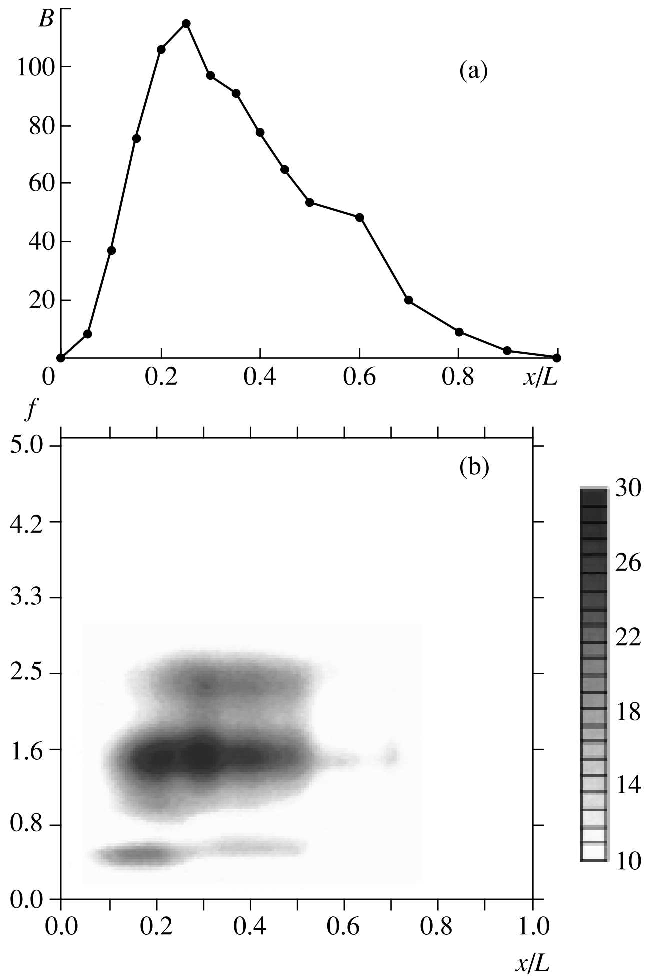

Fig. 2. (a) The plot of a total bicoherency B versus spatial coordinate x for the signals $h(t) = a\sin(2\pi f_0 t)$ and $g(t) = \varphi(t, x)$; (b) the projection of a bicoherent sum $B_\Sigma(x/L, f)$ constructed for the potential oscillations in various sections of the diode gap (different B_Σ values are represented by variable intensity of the projection color.

of chaotic oscillations. Figures 1a and 1b show the power spectra $P(f)$ (plotted in a nonlogarithmic scale), phase portraits (reconstructed using the Takens method [11]), and time variation of the electric field potential $\varphi(t)$ (Fig. 1a) and space charge density $\rho(t)$ (Fig. 1b) in the region of oscillating VC ($x/L = 0.25$). As can be seen, the temporal dynamics of the system is strongly irregular. The potential oscillations in the VC region show a more regular pattern as compared to that of the space charge density: the $\varphi(t)$ spectrum has a base frequency (f_0) and the phase portrait exhibits a structure related to the phase trajectory rotation with a time scale of $T \approx 1/f_0$. For this reason, we will use the $\varphi(t)$ oscillations for an analysis of processes in the system studied. It should be noted that the base frequency f_0 of the power spectrum is the same for oscillations in various diode cross sections.

Let us determine the total bicoherency (3) of data for the potential oscillations in vacuous diode sections x and a harmonic signal with a frequency corresponding to the base frequency f_0 of the power spectrum. This implies that we select signal h in relation (1) in the form of $a\sin 2\pi f_0 t$, while signal g represents the potential oscillations $\varphi(t, x)$. The calculations were performed using a base wavelet transformation of the Morlet type [12], which provides for a convenient interpretation of the results [4]. The results of calculations of the total bicoherency $B(x)$ as a function of the coordinate x are presented in Fig. 2a. As can be seen, the maximum total bicoherency (i.e., the maximum phase coupling between potential oscillations and the main time scale dynamics in the system) corresponds to the potential oscillations in the region of $x/L \approx 0.25$. This result implies that the basic spatiotemporal structure determining the main features in behavior of the system is localized at $x/L \sim 0.25$.

Now let us calculate the bicoherency sum $B_\Sigma(f)$ according to (2) using the spatiotemporal data for the potential oscillations in the diode gap. The signal h is selected in the form of potential oscillations $\varphi(t, 0.25/L)$ in the region of maximum total bicoherency (Fig. 2a) and the signal g represents the potential oscillations $\varphi(t, x)$ in various sections of the diode gap. The results are presented in Fig. 2b in the form of a projection of the B_Σ surface onto the coordinate plane (x, f), where x is the diode section coordinate and f is the frequency for which the bicoherency sum is determined. Different values of the function of two variables $B_\Sigma(x, f)$ in Fig. 2b are represented by variable intensity of the projection color. As can be seen, the $B_\Sigma(x, f)$ surface contains two clearly distinguished regions where the wavelet bicoherency sharply increases. On the (x, f) plane, these regions are located in the vicinity of $x \sim 0.2$–0.4, $f \sim 1.6$ and $x \sim 0.1$–0.15, $f \sim 0.4$. The magnitude of bicoherency in the first of these regions is significantly greater than that in the second region. The two regions can be related to two coherent structures determining the electron beam dynamics in the system studied. Using the data obtained, it is possible to estimate the characteristic time scales and spatial localization of these structures.

In order to verify the results of the bicoherent wavelet analysis, we have studied physical processes in an electron beam (see also [6]). Figure 1c shows a spatiotemporal diagram of the electron beam dynamics under the condition studied, in which each curve represents a charged particle trajectory. The diagram extends over three characteristic periods of the VC oscillations, which corresponds to a time interval of $t \sim 3/f_0$. As can be seen, for large n values, the VC forms outside the ion layer and permanently exists in the flow. The minimum potential depth performs irregular oscillations at a base frequency f_0. At the same time, a potential well is formed between the injection plane and VC, with an extremum at $x \sim 0.1$. This well traps either particles reflected from VC (and possessing small velocity on approaching the exit plane) or injected particles having lost the initial velocity in a strong retarding VC field. Trapped particles oscillating in the potential well are clearly distinguished on the spatiotemporal diagram (see Fig. 1c, where the trapped particle trajectory is depicted by a thick solid line). Thus, the beam features the formation of two electron bunches representing two self-sustained structures: VC proper and a metastable structure comprised of long-lived particles occurring in the interaction space, trapped in the potential well between the injection plane and VC. The spatial localization and characteristic time scales of both structures coincide with those determined by methods of the bicoherent wavelet transformation.

It should be noted that the spatiotemporal dynamics of the system studied is similar to the flow dynamics in a generator with VC of the triode type [7, 13, 14], which also exhibits a two-humped potential profile. The flow features a self-sustained vortex structure of trapped particles. The interaction between VC and this vortex gives rise to complicated flow dynamics analogous to that described in [15].

Thus, the chaotic dynamics and structure formation in an electron beam with virtual cathode in a diode with strongly inhomogeneous ion background were analyzed by the bicoherent wavelet transformation method. Using this method for the analysis of spatiotemporal data, it is possible to effectively reveal coherent structures determining the dynamics of systems featuring developed spatial chaos.

Acknowledgments. This study was supported by the Russian Foundation for Basic Research, project no. 01-02-17392.

REFERENCES

1. B. Ph. Van Milligen, E. Sánchez, T. Estrada, *et al.*, Phys. Plasmas **2** (8), 3017 (1995).
2. N. M. Astaf'eva, Usp. Fiz. Nauk **166** (11), 1145 (1996) [Phys. Usp. **39**, 1085 (1996)].
3. *Wavelets in Physics*, Ed. by J. C. Van den Berg (Cambridge Univ. Press, Cambridge, 1998).
4. V. G. Anfinogentov, A. A. Koronovskiĭ, and A. E. Khramov, Izv. Akad. Nauk, Ser. Fiz. **64** (12), 2383 (2000).
5. V. G. Anfinogentov and A. E. Khramov, Pis'ma Zh. Tekh. Fiz. **24** (21), 74 (1998) [Tech. Phys. Lett. **24**, 860 (1998)].
6. V. G. Anfinogentov and A. E. Khramov, Izv. Akad. Nauk, Ser. Fiz. **62** (12), 2428 (1998).
7. V. D. Selemir, B. V. Alekhin, V. E. Vatrunin, *et al.*, Fiz. Plazmy **20** (7, 8), 689 (1994) [Plasma Phys. Rep. **20**, 621 (1994)].
8. *High Power Microwave Sources*, Ed. by V. L. Granatstein and I. Alexeff (Artech House, Boston, 1987), Chap. 13.
9. C. K. Bridsall and A. B. Langdon, *Plasma Physics, Via Computer Simulation* (McGraw-Hill, New York, 1985).
10. A. M. Afonin, A. N. Didenko, A. F. Pautkin, and A. S. Roshal', Radiotekh. Élektron. (Moscow) **37** (10), 1889 (1992).
11. F. Takens, in *Lectures Notes in Mathematics, Warwick 1980*, Ed. by D. Rand and L.-S. Young (Springer-Verlag, New York, 1981), p. 366.
12. A. Grossmann and J. Mortel, SIAM J. Math. Anal. **15**, 723 (1984).
13. V. P. Grigor'ev, A. G. Zherlitsyn, and T. V. Koval', Fiz. Plazmy **16**, 1353 (1990) [Sov. J. Plasma Phys. **16**, 784 (1990)].
14. A. P. Privezentsev and G. P. Fomenko, Izv. Vyssh. Uchebn. Zaved., Ser. Prikl. Nelineĭnaya Din. **2** (5), 56 (1994).
15. V. G. Anfinogentov and A. E. Khramov, Izv. Vyssh. Uchebn. Zaved., Ser. Prikl. Nelineĭnaya Din. **6** (1), 93 (1998).

Translated by P. Pozdeev

SPELL: vircator